

Nonadditivity in the effective interactions of binary charged colloidal suspensions

This article has been downloaded from IOPscience. Please scroll down to see the full text article.

2009 J. Phys.: Condens. Matter 21 424117

(<http://iopscience.iop.org/0953-8984/21/42/424117>)

View [the table of contents for this issue](#), or go to the [journal homepage](#) for more

Download details:

IP Address: 129.252.86.83

The article was downloaded on 30/05/2010 at 05:35

Please note that [terms and conditions apply](#).

Nonadditivity in the effective interactions of binary charged colloidal suspensions

E Allahyarov^{1,2,3} and H Löwen¹

¹ Institut für Theoretische Physik II: Weiche Materie, Heinrich-Heine-Universität Düsseldorf, Universitätsstraße 1, D-40225 Düsseldorf, Germany

² Department of Physics, Case Western Reserve University, Cleveland, OH 44106, USA

³ Joint Institute for High Temperatures, Russian Academy of Sciences, Moscow, Russia

E-mail: elshad.allakhyarov@case.edu

Received 10 March 2009, in final form 20 April 2009

Published 29 September 2009

Online at stacks.iop.org/JPhysCM/21/424117

Abstract

Based on primitive model computer simulations with explicit microions, we calculate the effective interactions in a binary mixture of charged colloids with species A and B for different size and charge ratios. An optimal pairwise interaction is obtained by fitting the many-body effective forces. This interaction is close to a Yukawa (or Derjaguin–Landau–Verwey–Overbeek (DLVO)) pair potential but the AB cross-interaction is different from the geometric mean of the two direct AA and BB interactions. As a function of charge asymmetry, the corresponding nonadditivity parameter is first positive, then significantly negative and is then positive again. We finally show that an inclusion of nonadditivity within an optimal effective Yukawa model gives better predictions for the fluid pair structure than DLVO theory.

(Some figures in this article are in colour only in the electronic version)

1. Introduction

Phase diagrams and structural correlations in binary mixtures are much richer than those of their one-component counterparts [1] since there are additional thermodynamic degrees of freedom. Understanding the phase behaviour from first principles [2, 3] requires a knowledge of the effective interaction forces between the different species which is—in general—a many-body force. Even if this interaction is pairwise additive, the full calculation of structure and phase behaviour has only been done for selected cases. Among those are hard spheres [4–7], oppositely charged colloids [8, 9], two-dimensional dipolar mixtures [10, 11] and two-dimensional Yukawa mixtures [12].

In this paper we consider a three-dimensional binary colloidal suspension of two species A and B of charged spheres ('macroions') with different charges ($Z_A e$ and $Z_B e$, e denoting the electron charge) and diameters (σ_A and σ_B) [13–15]. The traditional Derjaguin–Landau–Verwey–Overbeek (DLVO) theory describes the interaction between the two species as an effective pairwise Yukawa potential [16, 17]

$$V(r) = \frac{Z_i e}{1 + \sigma_i \kappa_D / 2} \frac{Z_j e}{1 + \sigma_j \kappa_D / 2} \frac{\exp(-\kappa_D(r - (\sigma_i + \sigma_j)/2))}{\epsilon r} \quad (1)$$

where $(ij) = (AA), (AB), (BB)$, ϵ denotes the dielectric constant of the solvent and κ_D is the Debye–Hückel screening parameter. The latter is given as

$$\kappa_D^2 = 4\pi \left(\sum_j z_j^2 \rho_j \right) / \epsilon k_B T \quad (2)$$

where the sum runs over all microions with their charges z_j and partial number densities ρ_j . The DLVO theory is a linearized theory and therefore neglects nonlinear screening effects [19, 18] which give rise to effective many-body forces [20–24]. Nonlinear effects can at least partially be accounted for by charge renormalization which is conveniently calculated in a spherical Poisson–Boltzmann cell model [25]. The cell approach was recently generalized towards binary mixtures by Torres *et al* [26]. In the latter approach, it was shown that charge renormalization is different for the different species such that the ratio of effective charges is different from that of the bare charge. However, the cross-interaction was not addressed in this study.

The importance of the cross-interaction between A and B relative to the direct part AA and BB determines the so-called nonadditivity parameter Δ of the mixture which is crucial for the topology of phase diagrams. Binary hard sphere

systems have been studied as a prototype for any nonadditive mixtures [27–29]. In general, a positive nonadditivity is realized if the cross-interaction is more repulsive than the mean of the two direct interactions. For high positive nonadditivity ($\Delta > 0$), macrophase separation into an A-rich and B-rich phase is observed, i.e. the system minimizes the interface where the AB cross-interactions play a dominant role. The other case of negative nonadditivity ($\Delta < 0$) implies a weaker cross-interaction in terms of the bare ones such that the system tends to mix and to exhibit micro-phase-separation [30].

For pairwise Yukawa interactions $V_{ij}(r) = Z_{ij}^* \exp(-\kappa_D r)/r$ ($(i, j) = (AA), (AB), (BB)$), a dimensionless nonadditivity parameter Δ can be quantified by invoking the deviation of an ideal Berthelot mixing rule [31, 32] via the relation

$$1 + \Delta = Z_{12}^{*2}/Z_{11}^* Z_{22}^*. \quad (3)$$

For charged suspensions, classical DLVO theory (see equation (1)) implies a vanishing Δ since the effective charges are the same in all interactions. There are other realizations of a binary Yukawa system in dusty plasmas [33–35] and metallic mixtures [36] or amorphous silica [37]. In fact, the binary Yukawa model has been widely used and employed to investigate effective interactions [38], fluid–fluid phase separation [31, 39, 40], vitrification [41–45] and transport properties [46]. In most studies of binary Yukawa systems, the nonadditivity parameter is set to zero, except for [31, 32] where the effect of positive nonadditivity Δ on fluid–fluid phase separation is considered. In the context of dusty plasmas, there is another recent study showing that the nonadditivity parameter Δ is positive in general [47]. This leads to macrophase separation in binary dusty plasmas, as observed in experiments [35, 47]. The physical origin of the interaction in dusty plasmas, however, is different from that relevant for charged colloidal suspensions. While for the former the ions are described by a Gurevich distribution, a Boltzmann distribution is appropriate for the latter.

In this paper, we focus on the nonadditivity of the cross-interaction for charged colloidal suspensions. Using computer simulations with explicit microions [48–51], we calculate the effective interactions in a charged binary mixture and find that the sign of the nonadditivity depends on the parameters, in particular on the charge asymmetry. The nonadditivity parameter is calculated first by using simulations of three pairs of macroions, namely AA, AB and BB in a periodically repeated simulation box at fixed screening. We also consider larger systems with 24 macroions at different compositions in order to check the effect on many-body forces on Δ . In the latter case we fit the many-body forces by effective pairwise forces $-dV_{ij}(r)/dr$ and extract Δ from the optimal fit [52]. We confirm that Δ is unchanged. Our main findings are (i) that Δ is typically large and cannot be neglected and (ii) that the sign of Δ depends on the parameters such as charge asymmetry. If a binary charged colloidal mixture is described by an effective Yukawa model, Δ needs to be incorporated into the description. For instance when compared to DLVO theory, a much better description of the fluid pair structure is achieved within an effective Yukawa model and non-vanishing Δ .

The paper is organized as follows: in section 2 we describe the model and the simulation method and apply it to the case of two macroions. Many-body simulations with 24 macroions are discussed in section 3. Then we present data for a large system with effective pairwise Yukawa forces in order to see the effect of non-vanishing nonadditivity in section 4. Finally we conclude in section 5.

2. Simulations with two macroions

We model all ions as uniformly charged hard spheres such that they are interacting via excluded volume and Coulomb forces which are reduced by the dielectric constant ϵ of the solvent. The two species of charged colloids have a mesoscopic hardcore diameter σ_A (respectively σ_B) and a total charge $Z_A e$ (respectively $Z_B e$) while all microions are monovalent with a charge e (e denoting the electron charge) and a microscopic hardcore diameter σ_c . For finite salt concentrations, there are both counter and coions in the solution and the microscopic core of oppositely charged microions is needed to prevent the system from Coulomb collapse. The averaged concentration of added salt is denoted with n_s . The salt is always monovalent. The system is kept at room temperature T such that the Bjerrum length for the microions is $\lambda_B = e^2/\epsilon k_B T = 7.8 \text{ \AA}$ with $\epsilon = 80$ the dielectric constant of water at room temperature.

A cubic simulation box of edge length L with periodic boundary conditions is used containing two macroions and the following three cases are studied separately: (i) two A macroions, (ii) two B macroions and (iii) one A and one B macroion. The two macroions are placed along the room diagonal of the simulation box and possess a fixed central distance r . At fixed macroion positions, the microions are moved by constant temperature molecular dynamics and the averaged force F acting on the two macroions is calculated. The latter fulfils Newton’s third law. For more technical details we refer the reader to [48, 49, 53–56]. Then the distance r is varied and the force–distance curve $F(r)$ is gained.

Inspired by the DLVO expression (1), we anticipate that the screening length will not differ much in the three cases (i), (ii), (iii) and that it will be comparable to the Debye–Hückel expression. This assumption will be tested and justified later by a many macroion simulation reported in section 3. Therefore we adjust the box length in the three cases in order to reproduce the same Debye–Hückel screening length (2).

Results for the distance-resolved forces $F(r)$ are shown in figures 1–3 for the three cases (i), (ii) and (iii) for extremely dilute macroion suspension with a packing fraction $\eta = 0.005$. Such a dilute case is chosen to diminish the boundary effects of the simulation box on the interaction forces. The parameters used are $\sigma_A = 1220 \text{ \AA}$, $\sigma_B = 680 \text{ \AA}$, $Z_A = 580$, and $Z_B = 330$. The prescribed inverse screening length κ_D in equation (2) depends on simulation box size L through the microion number density $\rho_j = N_j/L^3$, where N_j is the total number of microions of sort j , $j = +, -$, in the simulation box. This parameter is $\kappa_D \sigma_A = 0.8$ corresponding to box lengths of $L = 6.24\sigma_A$ (for (i)), $L = 5.72\sigma_A$ (for (ii)) and $L = 6.0\sigma_A$ (for (iii)). The obtained data for the distance-resolved forces $F(r)$

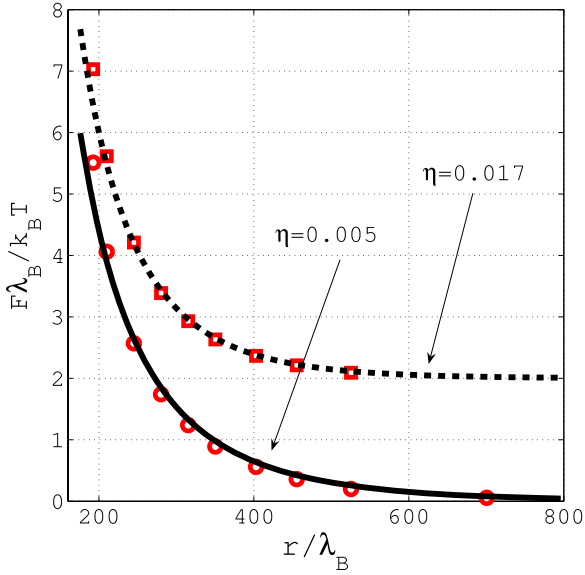


Figure 1. Dimensionless interaction force $F\lambda_B/(k_B T)$ for case (i) (AA macroion pair) as a function of dimensionless separation distance r/λ_B . Symbols denote the simulation data, the full curves are the Yukawa fit for two macroion packing fractions $\eta = 0.005$ (solid line) and $\eta = 0.017$ (dashed line, shifted upward). The fit data are given in the text.

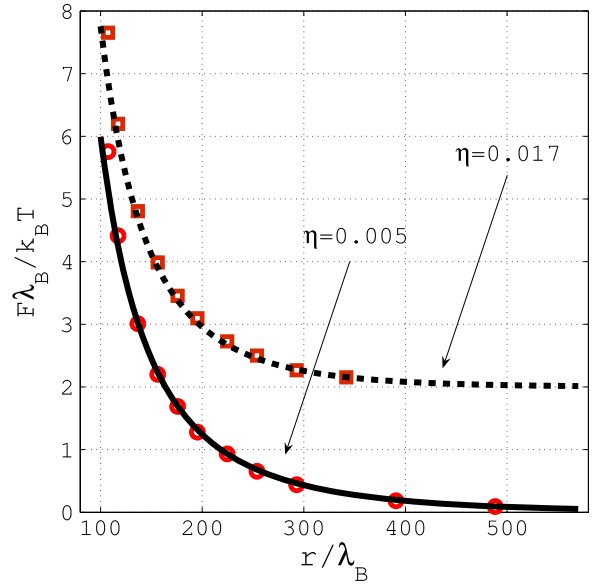


Figure 2. Dimensionless interaction force $F\lambda_B/(k_B T)$ for case (ii) (BB macroion pair) as a function of a dimensionless separation distance r/λ_B . Symbols denote the simulation data, the full curves are the Yukawa fit for two macroion packing fractions $\eta = 0.005$ (solid line) and $\eta = 0.017$ (dashed line, shifted upward). The fit data are given in the text.

were fitted with the Yukawa expression $Z_{ij}^* e^2 / (\epsilon r) (1/r + \kappa) \exp(-\kappa r)$ with $(ij) = (AA), (AB), (BB)$. The screening parameter κ and the three effective charge numbers Z_{AA}^* , Z_{BB}^* and Z_{AB}^* are used as fit parameters. We obtain $\kappa\sigma_A = 0.81$ (very close to its Debye–Hückel expression) and effective charge numbers of $Z_{AA}^* = 470$, $Z_{BB}^* = 260$, and $Z_{AB}^* = 330$ such that the nonadditivity parameter is negative:

$$\Delta = (Z_{AB}^*)^2 / (Z_{AA}^* Z_{BB}^*) - 1 = -0.11. \quad (4)$$

In a similar manner we calculate the interaction forces and Yukawa fitting parameters for another packing fraction $\eta = 0.017$ at which the images of macroions in neighbouring cells start to affect the long-range macroion–macroion interactions. We obtain $\kappa_D\sigma_A = 1.15$ and effective charge numbers of $Z_{AA}^* = 505$, $Z_{BB}^* = 265$, and $Z_{AB}^* = 342$ such that the nonadditivity parameter is $\Delta = -0.13$.

The results for extremely dilute $\eta = 0.005$ and dilute $\eta = 0.017$ cases shown in figures 1–3 which reveal that first of all, the Yukawa expression for the forces is an excellent fit over the relevant distance range explored. Moreover, while the screening parameter is very close to its Debye–Hückel expression, the nonadditivity of 11–13% is significant, i.e. a fit with imposed vanishing nonadditivity would result in a significantly worse force fit (by about 20%).

Next we explore the dependence of Δ on the charge asymmetry $\alpha = Z_A/Z_B$ by changing it in the range from 0 to 1 while keeping the size asymmetry $\sigma_A/\sigma_B = 1.8$ unchanged. In detail, we consider the B-charges $Z_B = 0, 100, 330, 580$ with fixed $Z_A = 580$ and $\kappa_D\sigma_A = 0.8$. Using the same simulation technique and fitting procedure, we extract the nonadditivity parameter Δ according to equation (4). The

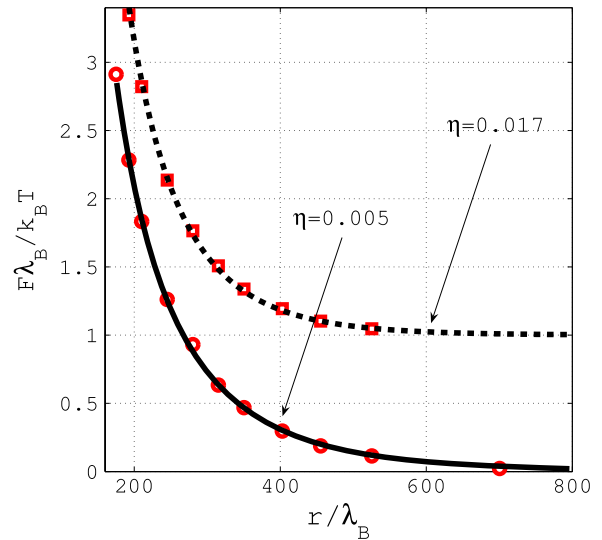


Figure 3. Dimensionless interaction force $F\lambda_B/(k_B T)$ for case (iii) (pair of A and B macroions) as a function of a dimensionless separation distance r/λ_B . Symbols denote the simulation data, the full curves are the Yukawa fit for two macroion packing fractions $\eta = 0.005$ (solid line) and $\eta = 0.017$ (dashed line, shifted upward). The fit data are given in the text.

results are presented in figure 4. The nonadditivity parameter Δ shows a clear non-monotonicity as a function of Z_B starting from positive values and turning to negative ones and back to positive ones as Z_B is increasing. For $Z_B = 0$, the BB interaction is small, but the AB interaction has still a repulsive contribution from entropic contact force [50] which drives Δ altogether towards a positive value. More intuitively, in the

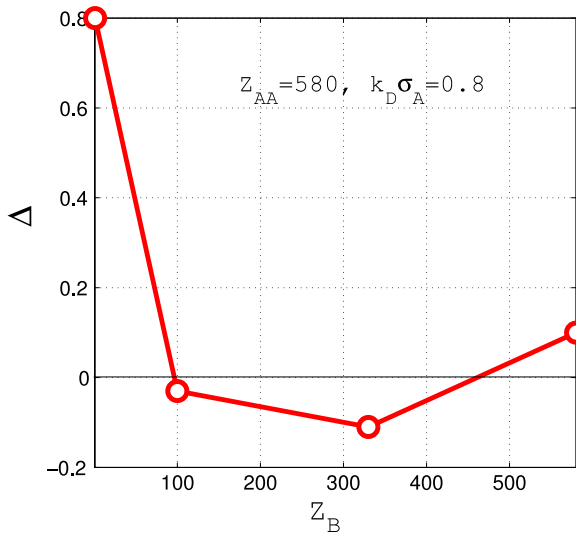


Figure 4. Nonadditivity parameter Δ for different charges Z_B at a fixed charge $Z_A = 580$.

case $Z_B = 0$, the AB interaction is dominated by the fact that more counterions are close to the charged A particle. It is better to exclude the uncharged B particle from the charged A particle in order to minimize the counterion energy. Therefore the AB interaction is repulsive. The other cases are less intuitive and we do not have a simple argument for the sign of Δ .

We have finally considered also the case of size-symmetric ($\sigma_A = \sigma_B$) but charge-asymmetric $Z_A/Z_B = 1.76$ macroions at a fixed screening length of $\kappa_D \sigma_A = 0.8$. Here, the nonadditivity parameter Δ was found to be -0.01 , much smaller than for the corresponding size-asymmetric case with $\sigma_A/\sigma_B = 1.8$. Hence size asymmetry appears to be the more crucial input for the nonadditivity.

3. Simulations with many macroions

Let us now turn to a many-body simulation of the primitive model in a cubic cell containing altogether $N = N_A + N_B = 24$ macroions with different compositions $X = N_B/(N_A + N_B)$. The simulation box contains also $N_c = N_A Z_A + N_B Z_B$ oppositely charged counterions, and N_s salt ion pairs. The other parameters are as before if not otherwise stated. Six different macroion packing fractions were considered: $\eta = 0.017, 0.034, 0.12, 0.16, 0.23, 0.3$. For all simulations the salt concentration was kept constant at $n_s = 4 \times 10^{-6} \text{ mol l}^{-1}$. Now both the microions and the macroions are moved by constant temperature molecular dynamics. A simulation snapshot is shown in figure 5. After equilibration, we stored 200 statistically independent macroion configurations for each run. For each stored configuration, we averaged the total forces \vec{F}_i ($i = 1, N$) acting on the i th macroion over the microionic degrees of freedom. These forces are clearly many-body forces, in general. Following the idea of [52], we assign an optimal effective pair interaction by fitting all forces \vec{F}_i in all stored configurations by the same pairwise Yukawa interaction. As in section 2, the four fitting parameters are κ_D and the three

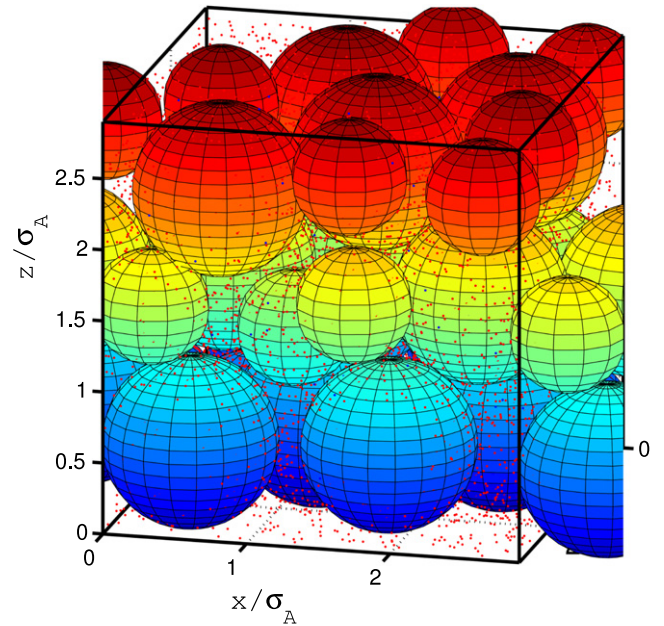


Figure 5. Full system snapshot picture for 24 macroions with equimolar composition $X = 1/2$. The system size is $2.9 \sigma_A$ at a total packing fraction of $\eta = 0.3$. The positively charged counter- and salt-ions (red online, at the top in the printed edition) and the negative salt-ions (blue online, at the bottom in the printed edition) are shown as dots. A vertical brightness gradient (colour gradient online) has been used for macroion positions along the z -axis. The parameters are: $Z_A = 580, Z_B = 330$.

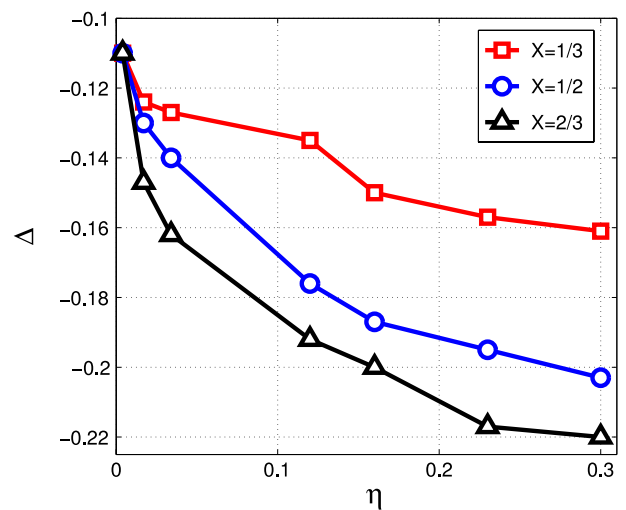


Figure 6. Nonadditivity parameter Δ as a function of a total macroion packing fraction η for three different compositions $X = 1/3, 1/2, 2/3$.

effective charge numbers Z_{AA}^*, Z_{BB}^* and Z_{AB}^* which determine the nonadditivity Δ directly.

The results of the optimal fit for $\Delta, Z_{AA}^*, Z_{BB}^*$ and $\kappa_D \sigma_A$ are shown in figures 6–9 as a function of the varied macroion volume fraction η for three different compositions $X = 1/3, 1/2, 2/3$.

The nonadditivity shown in figure 6 is clearly negative and decreases with increasing packing fraction. This trend can be intuitively understood since asymmetries are amplified

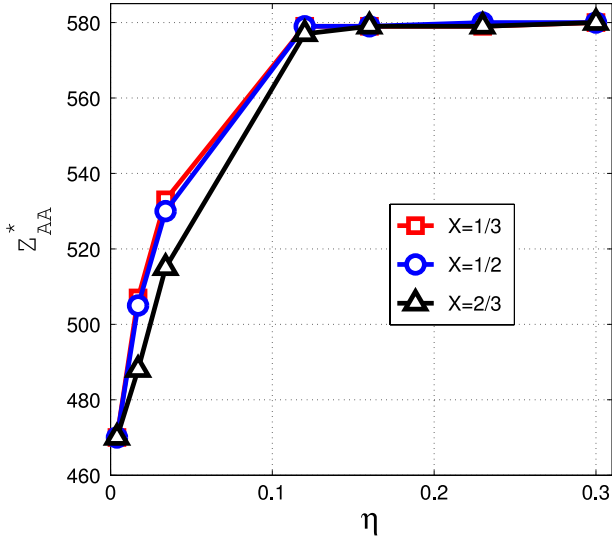


Figure 7. Optimal effective AA charge number Z_{AA}^* as a function of a total macroion packing fraction η for three different compositions $X = 1/3, 1/2, 2/3$.

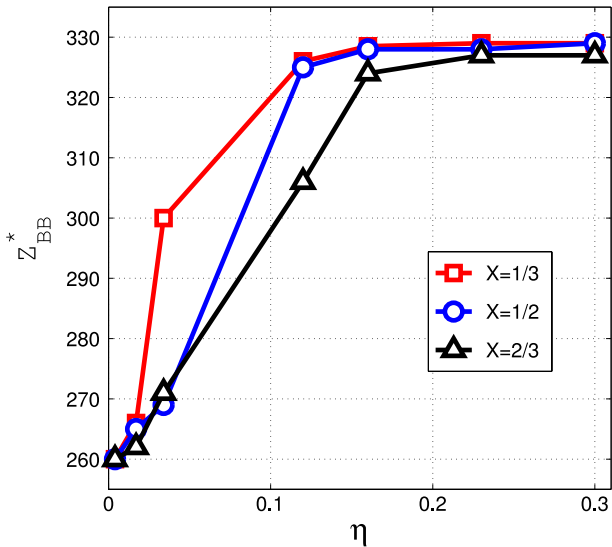


Figure 8. Optimal effective BB charge number Z_{BB}^* as a function of a total macroion packing fraction η for three different compositions $X = 1/3, 1/2, 2/3$.

if one approaches smaller interparticle distances. A second important conclusion from figure 6 is that the many-body simulations yield the *same* value for Δ as those obtained from the simulations of pairs in section 2. In fact, the value $\Delta = -0.13$ is reproduced at low volume fractions $\eta = 0.017$. The effective charges and screening length deduced from pair macroion simulations for $\eta = 0.017$ perfectly fit the simulation data for many macroions at the same packing fraction η for the macroions. The effective charge numbers Z_{AA}^* and Z_{BB}^* shown in figures 7 and 8 increase slightly with volume fraction, which is the standard trend also for one-component charged suspensions [57, 58]. The screening constant shown in figure 9 increases with η , following the same trend as its Debye–Hückel expression which is also indicated in figure 9.

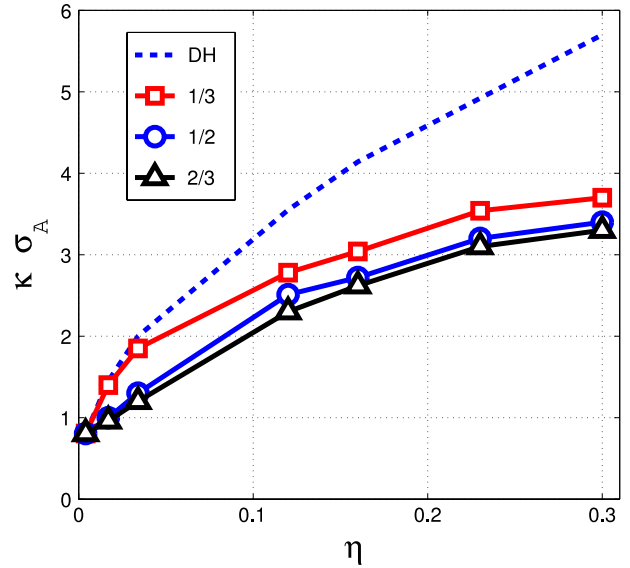


Figure 9. Optimal screening parameter $\kappa\sigma_A$ as a function of a total macroion packing fraction η for three different compositions $X = 1/3, 1/2, 2/3$. The dashed line is the Debye–Hückel value of screening in the simulated system according to equation (2) in the text.

4. Simulations using the optimal effective Yukawa interaction

We finally explore the impact of a non-vanishing Δ on the fluid structure of binary charged suspensions. In doing so we make use of the optimal effective Yukawa fit gained in section 3 and use it as an input in classical coarse-grained binary Yukawa simulations (without any microions). In detail, classical molecular dynamics simulations for a mixture of similarly charged A and B big particles were carried out. These simulations can be done for much larger systems and we included 1000 A and 1000 B particles at equimolar composition. Two volume fractions are considered, a dilute system with $\eta = 0.034$ and a dense system where $\eta = 0.3$.

The effective macroion charge numbers, the screening constant and the nonadditivity parameter were chosen from results described in section 3. In detail, for the dilute system: $Z_{AA}^* = 530$, $Z_{BB}^* = 269$, $\kappa_D\sigma_A = 1.3$, $\Delta = -0.14$, while for the dense system, $Z_{AA}^* = 580$, $Z_{BB}^* = 330$, $\kappa_D\sigma_A = 3.4$, $\Delta = -0.2$. At these parameters the system is in the fluid phase.

We have calculated the partial pair correlations g_{AA} , g_{BB} and g_{AB} for the large Yukawa substitute system and the smaller system with explicit microions. The results are presented in figures 10 and 11. There is good agreement for the dilute case, demonstrating that the Yukawa fit is reproducing the pair correlations. For the dense system, there is again agreement except for the location of the first peak in $g_{BB}(r)$. This could have to do with finite-size effects of the $N = 24$ primitive model systems which are expected to get more prominent at high packing fractions.

As a reference we have also performed Yukawa simulations with effective interactions based on two effective charges Z_{AA}^* and Z_{BB}^* but where Δ is set to zero, i.e. where

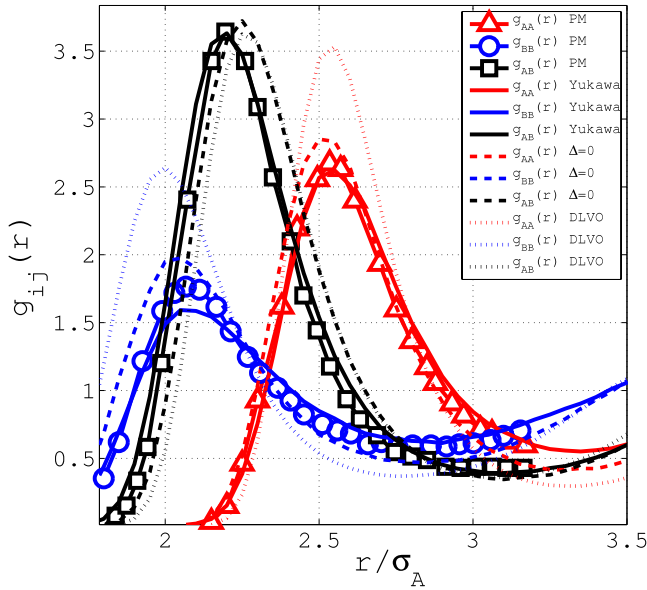


Figure 10. Partial macroion–macroion pair correlation functions for both the full primitive model (symbols) and the substitute Yukawa system (full lines) for a total packing fraction $\eta = 0.034$ at composition $X = 1/2$. The Yukawa simulations were carried for $\Delta = -0.14$, $\kappa_D\sigma_A = 1.3$, $Z_{AA}^* = 530$, $Z_{BB}^* = 269$. The additive Yukawa system results for $\Delta = 0$ and the same $\kappa_D\sigma_A$, Z_{AA}^* , Z_{BB}^* are given as dashed lines. The DLVO predictions are included as dotted lines.

$Z_{AB}^{*2} = Z_{AA}^*Z_{BB}^*$. The differences in the pair structure are pointing to the importance of nonzero nonadditivity. There are even more deviations of the fluid pair structure when the simple DLVO expression is taken, which significantly overestimates the structure, see the dotted lines in figures 10 and 11. One of the main conclusions therefore is that one has to be careful if Δ for binary charged suspensions is neglected.

5. Concluding remarks

In conclusion we have determined the nonadditivity parameter in binary charged suspensions by primitive model computer simulations with explicit macroions and found significant deviations from zero. The sign depends on the actual parameter combination, in particular on the charge asymmetry. This implies that a realistic modelling of charged suspensions on the effective pairwise Yukawa level should incorporate a non-vanishing Δ .

A priori an intuition for the sign of Δ is difficult. Intuition only works in limiting cases. For example, in the depletion limit of many small macroions and few big ones there is attraction between the big ones which would result in a positive Δ .

In the future, more detailed investigations are planned to explore the full parameter space better. It would be interesting to calculate the effective interaction in the solid phase relative to the coexisting fluid phase.

In inhomogeneous situations like sedimentation in a gravitational field, binary suspensions have been examined by primitive model computer simulations [59] and a simple

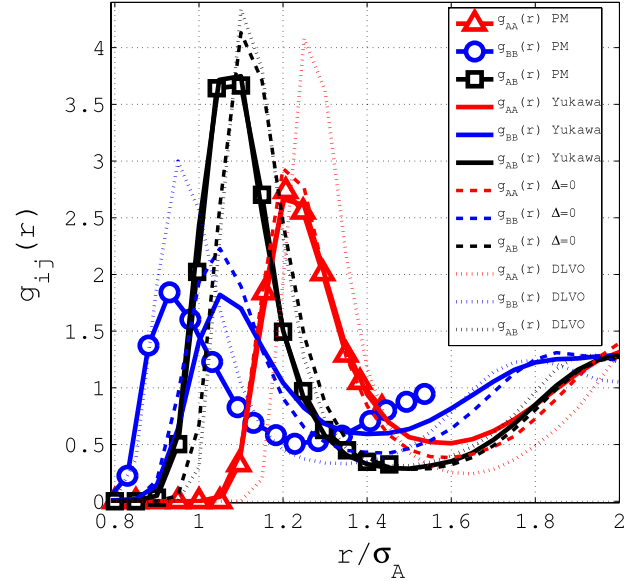


Figure 11. Partial macroion–macroion pair correlation functions for both the full primitive model (symbols) and the substitute Yukawa system (full lines) for a total packing fraction $\eta = 0.3$ at composition $X = 1/2$. The Yukawa simulations were carried out for $\Delta = -0.2$, $\kappa_D\sigma_A = 3.4$, $Z_{AA}^* = 580$, $Z_{BB}^* = 330$. The additive Yukawa system results for $\Delta = 0$ and the same $\kappa_D\sigma_A$, Z_{AA}^* , Z_{BB}^* are given as dashed lines. The DLVO predictions are included as dotted lines.

binary Yukawa pairwise interaction model was found to be inappropriate [60]. Since in our bulk simulation the pairwise Yukawa model was a good fit, we expect that this is due to the density gradient in the system but this will require more detailed studies.

Binary suspension can be prepared in a controlled way [61, 62] and their structural correlation, dynamics and phase diagrams can be explored. Depending on the size and charge ratio different freezing diagrams (azeotropic, spindle, eutectic) [63–66] have been obtained in the experiments. Since the nonadditivity Δ depends on the composition, this might point to the fact that details of the variation of Δ with composition and also with the phases itself (fluid or crystal) determine the shape of the freezing diagrams. Finally it would be interesting to study nonadditivity effects in charged mixtures of rods [67] or rod and sphere mixtures. It would also be interesting to explore the effect of multivalent counterions which could lead to mutual attraction [49, 68].

Acknowledgments

We thank T Palberg and A V Ivlev for helpful discussions. This work was supported by the DFG via the SFB TR6 (project D1).

References

- [1] Tammann G 1913 *Ann. Phys.* **40** 237
- [2] Hafner J 1987 *From Hamiltonians to Phase Diagrams* (Berlin: Springer)
- [3] Gompper G and Schick M 2006 *Complex Colloidal Suspensions (Soft Matter vol 2)* (Weinheim: Wiley–VCH)

- [4] Pronk S and Frenkel D 2003 *Phys. Rev. Lett.* **90** 255501
- [5] Xu H and Baus M 1992 *J. Phys.: Condens. Matter* **4** L663
- [6] Eldridge M D, Madden P A and Frenkel D 1993 *Nature* **365** 35
- [7] Bartlett P, Ottewill R H and Pusey P N 1992 *Phys. Rev. Lett.* **68** 3801
- [8] Leunissen M E, Christova C G, Hynninen A P, Royall C P, Campbell A I, Imhof A, Dijkstra M, van Roij R and van Blaaderen A 2005 *Nature* **437** 235
- [9] Hynninen A P, Christova C G, van Roij R, van Blaaderen A and Dijkstra M 2006 *Phys. Rev. Lett.* **96** 138308
- [10] Assoud L, Messina R and Löwen H 2007 *Europhys. Lett.* **80** 48001
- [11] Fornleitner J, Lo Verso F, Kahl G and Likos C N 2008 *Soft Matter* **4** 480
- [12] Assoud L, Messina R and Löwen H 2008 *J. Chem. Phys.* **129** 164511
- [13] Hansen J-P and Löwen H 2000 *Annu. Rev. Phys. Chem.* **51** 209
- [14] Levin Y 2002 *Rep. Prog. Phys.* **65** 1577
- [15] Messina R 2009 *J. Phys.: Condens. Matter* **21** 113102
- [16] Mendez-Alcaraz J M, D'Aguanno B and Klein R 1991 *Physica A* **178** 421
- [17] Krause R, D'Aguanno B, Mendez-Alcaraz J M and Klein R 1991 *J. Phys.: Condens. Matter* **3** 4459
- [18] Löwen H, Hansen J P and Madden P A 1993 *J. Chem. Phys.* **98** 3275
- [19] Löwen H, Madden P A and Hansen J P 1992 *Phys. Rev. Lett.* **68** 1081
- [20] Löwen H and Allahyarov E 1998 *J. Phys.: Condens. Matter* **10** 4147
- [21] Wu J Z, Bratko D, Blanch H W and Prausnitz J M 2000 *J. Chem. Phys.* **113** 3360
- Wu J Z, Bratko D, Blanch H W and Prausnitz J M 1998 *J. Phys.: Condens. Matter* **10** 4147
- [22] Reinke D, Stark H, von Grünberg H H, Schofield A B, Maret G and Gasser U 2007 *Phys. Rev. Lett.* **98** 038301
- [23] Russ C, Brunner M, Bechinger C and Von Grünberg H H 2005 *Europhys. Lett.* **69** 468
- [24] Kreer T, Horbach J and Chatterji A 2006 *Phys. Rev. E* **74** 021401
- [25] Trizac E, Bocquet L, Aubouy M and von Grünberg H H 2003 *Langmuir* **19** 4027
- [26] Torres A, Téllez G and van Roij R 2008 *J. Chem. Phys.* **128** 154906
- [27] Roth R, Evans R and Louis A A 2001 *Phys. Rev. E* **64** 051202
- [28] Louis A A and Roth R 2001 *J. Phys.: Condens. Matter* **13** L777
- [29] Pellicane G, Saija F, Caccamo C and Giaquinta P V 2006 *J. Chem. Phys.* **110** 4359
- [30] Hoffmann N, Ebert F, Likos C N, Maret G and Löwen H 2006 *Phys. Rev. Lett.* **97** 078301
- [31] Hopkins P, Archer A J and Evans R 2006 *J. Chem. Phys.* **124** 054503
- [32] Hopkins P, Archer A J and Evans R 2008 *J. Chem. Phys.* **129** 214709
- [33] Vaulina O S and Dranzhevskii I E 2007 *Plasma Phys. Rep.* **33** 494
- [34] Kalman G J, Hartmann P, Donko Z and Rosenberg M 2004 *Phys. Rev. Lett.* **92** 065001
- [35] Sütterlin K R, Wysocki A, Ivlev A V, R ath C, Thomas H M, Rubin-Zuzic M, Goedheer W J, Fortov V E, Lipaev A M, Molotkov V I, Petrov O F, Morfill G E and L owen H 2009 *Phys. Rev. Lett.* **102** 085003
- [36] Kikuchi N and Horbach J 2007 *Europhys. Lett.* **77** 26001
- [37] Carre A, Berthier L, Horbach J, Ispas S and Kob W 2007 *J. Chem. Phys.* **127** 114512
- [38] Louis A A, Allahyarov E, L owen H and Roth R 2002 *Phys. Rev. E* **65** 061407
- [39] Sch oll-Paschinger E and Kahl G 2003 *J. Chem. Phys.* **118** 7414
- [40] K ofinger J, Wilding N B and Kahl G 2006 *J. Chem. Phys.* **125** 234503
- [41] L owen H, Hansen J P and Roux J N 1991 *Phys. Rev. A* **44** 1169
- [42] Chavez-Rojo M A and Medina-Noyola M 2006 *Physica A* **366** 55
- [43] Kikuchi N and Horbach J 2007 *Europhys. Lett.* **77** 26001
- [44] Chavez-Rojo M A, Juarez-Maldonado R and Medina-Noyola M 2008 *Phys. Rev. E* **77** 040401(R)
- [45] Juarez-Maldonado R and Medina-Noyola M 2008 *Phys. Rev. E* **77** 051503
- [46] Salin G and Gilles D 2006 *J. Phys. A: Math. Gen.* **17** 4517
- [47] Ivlev A V, Zhdanov S K, Thomas H M and Morfill G E 2009 *Europhys. Lett.* **85** 45001
- [48] D'Amico I and L owen H 1997 *Physica A* **237** 25
- [49] Allahyarov E, D'Amico I and L owen H 1998 *Phys. Rev. Lett.* **81** 1334
- [50] Allahyarov E, L owen H and Trigger S 1998 *Phys. Rev. E* **57** 5818
- [51] Allahyarov E, D'Amico I and L owen H 1999 *Phys. Rev. E* **90** 3199
- [52] L owen H and Kramposthuber G 1993 *Europhys. Lett.* **23** 637
- [53] L owen H, H artel A, Barreira-Fontecha A, Sch ope H J, Allahyarov E and Palberg T 2008 *J. Phys.: Condens. Matter* **20** 404221
- [54] Allahyarov E, L owen H, Louis A A and Hansen J-P 2002 *Europhys. Lett.* **57** 731
- [55] Allahyarov E, L owen H, Louis A A and Hansen J-P 2003 *Phys. Rev. E* **67** 051404
- [56] Allahyarov E, Zaccarelli E, Sciortino F, Tartaglia P and L owen H 2007 *Europhys. Lett.* **78** 38002
- [57] Diehl A, Barbosa M C and Levin Y 2001 *Europhys. Lett.* **53** 86
- [58] Denton A R 2008 *J. Phys.: Condens. Matter* **20** 494230
- [59] Esztermann A and L owen H 2004 *Europhys. Lett.* **68** 120
- [60] Torres A, Cuetos A, Dijkstra M and van Roij R 2008 *Phys. Rev. E* **77** 031402
- [61] Koenderink G H, Zhang H Y, Lettinga M P, N agele G and Philipse A P 2001 *Phys. Rev. E* **64** 022401
- [62] Stipp A and Palberg T 2007 *Phil. Mag. Lett.* **87** 899
- [63] Hunt W J and Zukoski C F 1999 *J. Colloid Interface Sci.* **210** 332
- [64] Meller A and Stavans J 1992 *Phys. Rev. Lett.* **68** 3645
- [65] Wette P, Sch ope H J and Palberg T 2005 *J. Chem. Phys.* **122** 144901
- [66] Lorenz N, Liu J N and Palberg T 2008 *Colloids Surf. A* **319** 109
- [67] L owen H 1994 *J. Chem. Phys.* **100** 6738
- [68] Allahyarov E, Gompper G and L owen H 2004 *Phys. Rev. E* **69** 041904